the FEBS Journal

Regulation of translational efficiency by different splice variants of the Disc large 1 oncosuppressor 5′-UTR

Ana L. Cavatorta[1], Florencia Facciuto[1], Marina Bugnon Valdano[1], Federico Marziali[1], Adriana A. Giri[1], Lawrence Banks[2] and Daniela Gardiol[1]

1 Instituto de Biología Molecular y Celular de Rosario – CONICET, Facultad de Ciencias Bioquímicas y Farmacéuticas, Rosario, Argentina
2 International Centre for Genetic Engineering and Biotechnology, Trieste, Italy

Keywords
cancer; DLG1; polarity; translation regulation; 5′-UTR

Correspondence
D. Gardiol, IBR-CONICET, Facultad de Ciencias Bioquímicas y Farmacéuticas, Suipacha 531, 2000 Rosario, Argentina
Fax: +54 341 4390645
Tel: +54 341 4350661
E-mail: gardiol@ibr.gov.ar

(Received 23 January 2011, revised 1 May 2011, accepted 17 May 2011)

doi:10.1111/j.1742-4658.2011.08188.x

Human Disc large (DLG1) has been demonstrated to be involved in the control of cell polarity and maintenance of tissue architecture, and is frequently lost in human tumours. However, the mechanisms controlling DLG1 expression are poorly understood. To further examine the regulation of DLG1 expression, we analysed the 5′ ends of DLG1 transcripts by rapid amplification of cDNA ends polymerase chain reaction. We identified an alternative splicing event in the 5′ region of DLG1 mRNA that generates transcripts with two different 5′ untranslated regions (5′-UTRs). We show by reporter assays that the DLG1 5′-UTR containing an alternatively spliced exon interferes with the translation of a downstream open reading frame (ORF). However, no significant differences in mRNA stability among the DLG1 5′-UTR variants were observed. Sequence analysis of the additional exon present in the larger DLG1 5′-UTR showed the presence of an upstream short ORF which is lost in the short version of the 5′-UTR DLG1. By mutagenesis and luciferase assays, we analysed the contribution of this upstream short ORF in reducing translation efficiency, and showed that its disruption can revert, to some extent, the negative regulation of large 5′-UTR. Using computational modelling we also show that the large DLG1 5′-UTR isoform forms a more stable structure than the short version, and this may contribute to its ability to repress translation. This represents the first analysis of the 5′ region of the DLG1 transcripts and shows that differential expression of alternatively spliced 5′-UTRs with different translational properties could result in changes in DLG1 abundance.

Introduction

Discs large 1 (DLG1/SAP97), a mammalian homologue of the *Drosophila* discs large (DLGA) protein, is a representative member of a family of scaffolding proteins termed membrane-associated guanylate kinase homologues. These proteins contain multiple protein domains including PSD-95/DLG/ZO-1 (PDZ) motifs that function as protein–protein interaction modules [1,2]. In *Drosophila*, DLGA was identified as a tumour suppressor and it was demonstrated to be involved in the regulation of both cell polarity and cell proliferation [3,4]. Moreover, inactivating mutations in the *DLGA* gene led to neoplastic overgrowth of imaginal discs [5]. Mammalian homologues of DLGA are functionally conserved and it has been postulated that they

Abbreviations
APC, adenomatous polyposis coli; DLGA, *Drosophila* discs large; DLG1, human disc large; HPV, human papillomavirus; LUC, firefly luciferase; PDZ, PSD-95/DLG/ZO-1 domains; qPCR, quantitative PCR; SDH, human succinate dehydrogenase; TSS, transcriptional start site; uORF, upstream ORF.

also have tumour suppressor activities. DLG1 is localized in the cytoplasm and at the adherens junctions of polarized epithelial cells [6,7] and, together with the Scribble and the Lg1 proteins, forms the Scrib lateral polarity complex, which has important roles in the establishment of apical–basal polarity [8].

DLG1 has the ability to interact with a variety of proteins through its PDZ domains. Interestingly, DLG1 binds to the adenomatous polyposis coli (APC) oncosuppressor and this DLG1–APC complex inhibits cell cycle progression in response to cell contact in epithelial cells, indicating a role for DLG1 in growth control [9]. In addition, DLG1 binds to the adenovirus E4-ORF1 protein, the human T-cell leukaemia virus type 1 Tax protein and the high risk human papillomavirus (HPV) E6 protein, and the tumourigenic potential of these viral oncoproteins depends, in part, on the ability to inactivate this cellular factor [10–12]. Moreover, high risk HPV E6 proteins can target DLG1 for ubiquitin-mediated degradation and this activity is absent in E6 proteins derived from low risk HPV [11,13,14].

Although the existing data support a role for DLG1 in tumour suppression, the actual contribution to human carcinogenesis is not fully understood. Several recent reports, however, showed a strong correlation between decreased expression of human DLG1 and tumour progression. Changes in the distribution and abundance of DLG1 were observed in gastric, cervical, breast and colon cancer during the different stages of tumour formation, with a loss of DLG1 expression being associated with complete lack of cell polarity and tissue architecture during the latest stages of malignant progression [15–19]. However, the molecular mechanisms regulating DLG1 expression, which may be responsible for the changes in its localization and abundance during carcinogenesis, are poorly understood.

Some post-translational modifications of DLG1 have been reported in epithelial cells, and they are mostly related to the control of DLG1 subcellular localization and functions. DLG1 has been shown to be post-translationally modified, under certain conditions, by the Jun N-terminal kinase, the P38γ MAP kinase, the cyclin-dependent kinases 1 and 2 and the PDZ-binding kinase, resulting in changes in distribution and stability of the protein [20–23]. Thus, alterations in the normal activity of these kinases might account for some of the changes in DLG1 expression observed during tumour development.

However, the loss of DLG1 observed in different cancers may be the result of different particular mechanisms, and transcriptional downregulation may also play an important role. Indeed, it was shown that in HPV-negative cervical cancer derived cells *DLG1* transcription levels were extremely low [24]. Nevertheless, very little is known about the molecular pathways that determine the transcriptional regulation of the human *DLG1* gene. We have therefore initiated studies to investigate the mechanisms that control *DLG1* gene expression; we have recently reported the cloning and functional analysis of a genomic 5′ flanking region of DLG1 ORF with promoter activity, and determined *cis* elements required for efficient transcription. We also demonstrated that the Snail family of transcription factors, which are repressors of several epithelial markers (such as E-cadherin, occludin, claudins and ZO-1) and inducers of the epithelial–mesenchymal transition [25], are involved in DLG1 downregulation [26].

To further examine the regulation of DLG1 expression, we analysed the 5′ ends of DLG1 transcripts by RACE-PCR and have identified an alternative splicing event in the 5′ region of DLG1 mRNA that generates transcripts with two different 5′-UTRs. A genome-wide screening of alternative splicing and transcriptional initiation estimated that a significant number of genes are differentially spliced within 5′-UTRs, and UTR heterogeneity for a specific gene is likely to have a differential impact on protein expression [27–29]. In this sense, many oncogenes and tumour suppressor genes tend to express atypically complex 5′-UTRs and it is thought that deregulation of translation, via these 5′-UTR sequences, is responsible for expression changes in cancer cells, playing a key role in carcinogenesis [30]. In this respect, Smith *et al*. recently reported that the efficiency of translation of oestrogen receptor isoforms (ERβ) is regulated by alternative 5′-UTRs. Moreover, the different ERβ 5′-UTRs are differentially expressed between normal and tumour tissues of breast and lung origin thereby resulting in changes in the levels of ERβ expression during carcinogenesis [31].

It is well established that translation control is mediated by 5′-UTRs that may influence the amount of protein produced from messages by altering mRNA stability, localization or translational efficiency [27,28]. Within 5′-UTRs, the presence of stable secondary structures, binding sites for trans-acting factors or short ORFs upstream (uORFs) of the main coding sequence can have a strong influence on cap-dependent translation [27]. Moreover, some factors that are known to reduce translation efficiency are longer 5′-UTRs with multiple start codons that may result in false starts or short ORF segments that lead to nonsense products [32–34]. In this work, we have shown by reporter assays that the DLG1 5′-UTR with an

alternatively spliced exon interferes with the translation of a downstream ORF, suggesting that the splicing event within the 5′-UTR contributes to regulation of DLG1 expression. We have also observed that the large version of the DLG1 5′-UTR generates stable secondary structures that may contribute to its ability to repress translation. The data presented in this study suggest that multiple mechanisms contribute to DLG1 regulation, and show that differential expression of alternative 5′-UTRs with different translational properties, in the total pool of DLG1 mRNAs, could result in changes in DLG1 abundance.

Results

Analysis of DLG1 mRNA 5′ region by RACE

Having previously reported the characterization and functional analysis of the DLG1 promoter region [26], we wanted to fully characterize the putative regulatory functions of the 5′ DLG1 sequences and determine whether the DLG1 transcriptional start site (TSS), identified using lymphocyte RNA, was conserved in epithelial tissue [35]. To do this, 5′ RACE reactions were carried out using RNA isolated from HaCaT cells that express high levels of DLG1 mRNA and specific *DLG1* primers (3′-DLG Outer and 3′-DLG Inner) as described in Materials and methods. These reactions yielded two bands of $\sim$ 150 and 250 bp as detected by gel analysis. The respective clones were sequenced and aligned with the published DLG1 gene sequence [35], and this analysis showed multiple transcription initiation sites spread throughout a region of $\sim$ 50 bp in exon A, located upstream of the previously reported TSS, arbitrarily designated as nucleotide +1 in our previous report [26] (Fig. 1A). This discrepancy may be due to cell-type-specific differences.

The products contained the 5′-UTR and part of exon C (containing the principal ATG), as predicted from the published cDNA sequence of DLG1 [35] (Fig. 1A). However, 5′ RACE experiments also revealed that the 5′-UTR of DLG1 undergoes differential splicing to produce two mRNA transcripts: a large one (5′-UTR DLG1 large), which contains 115 additional nucleotides designated as exon B; and a short version (5′-UTR DLG1 short) in which the exon B is absent (Fig. 1A). The additional 115 bp non-coding sequence, present in the 5′-UTR large version, matches exactly with the DLG1 cDNA, indicating that DLG1 contains two non-coding exons (exons A and B, Fig. 1A) and that exon B is alternatively spliced to produce two mRNA transcripts. It is important to point out that the original cDNA published by Lue *et al.* [35] coincided with the large 5′-UTR form. The extra exon B is flanked by AG and GT dinucleotides, so the splice junctions are consistent with the AG in the splice acceptor site and GT in the donor site (the GT–AG rule) [36] (Fig. 1B). However, analysis of the exon sequences at the splicing boundaries shows that even though the 3′ splice site matches perfectly with the mammalian consensus (GT), the 5′ site CG is not the optimal one (AG) (Fig. 1B). This could explain the fact that the splicing machinery can bypass the site, resulting in the large 5′-UTR species. There was no preferential use of a particular initiation start site for mRNA transcripts with or without exon B. Sequence analysis of the additional exon present in 5′-UTR DLG1 large showed the presence of a uATG followed by an in-frame termination codon upstream of the main DLG1 translation start site (Fig. 1B). This indicates the existence of a short uORF, which is lost in the short version of 5′-UTR DLG1.

With respect to species conservation, we examined the 5′-UTR of *Rattus norvegicus* DLG1 since it shares a 92% identity with human DLG1 at the protein level. The reported rat cDNA sequence (GeneBank ID U14950) showed little conservation with human DLG1 across the 5′-UTR; however, analysis of the sequence demonstrated the presence of consensus sites for a potential alternative splicing, and the presence of a uORF in the putative alternative spliced exon.

These findings seem to indicate that these alternative 5′-UTRs may play a role in regulating DLG1 expression. As a first step, we investigated if these alternative DLG1 5′-UTRs were expressed in different epithelial cell lines. We performed RT-PCR assays for the differential amplification of both 5′-UTRs, using RNA from different epithelial cell lines. To do this, we designed forward specific primers for each UTR and a reverse common primer matching sequence in exon C (Fig. 1A). As can be seen in Fig. 1C, both large and small 5′-UTR forms of DLG1, shown as upper and lower major bands respectively, could be detected in all cell lines analysed, validating the 5′ RACE results.

Different 5′-UTRs define the translational efficiency of the messages

To address the functional impact of these UTRs on the DLG1 mRNA transcripts, and their influence on the efficiency of translation of the subsequent ORF, we cloned each UTR immediately upstream of the firefly luciferase (LUC) cDNA in the pGL3-Promoter vector (pGL3P; Promega, Madison, WI, USA) (Fig. 2A). The two reporter constructs, designed as pGL3P-5′-UTR large and pGL3P-5′-UTR short, were

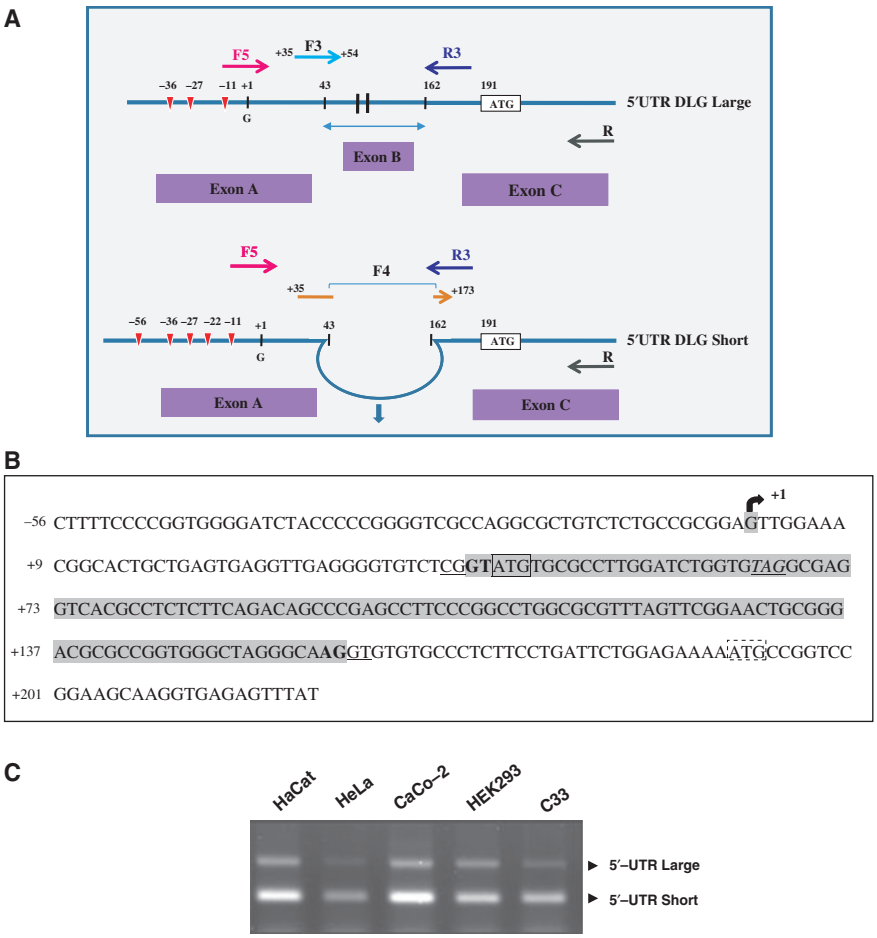

Fig. 1. The 5′-UTR of DLG1 undergoes differential splicing to produce two mRNA transcripts. (A) Schematic representation of 5′-UTR of DLG1 and mRNA splice variants. The multiple TSSs mapped by 5′-RACE-PCR, located upstream of the previously reported TSS (G) which is marked as +1 (GeneBank ID U13896 and U13897), are indicated by red arrowheads. Exons containing the 5′-UTR are indicated. The DLG 5′-UTR large includes exon A, exon B and part of exon C. In the short version of 5′-UTR DLG the exon B is absent. Location of primers used for specific PCR amplification of each alternative DLG1 5′-UTR (F3, F4 and R) and for cloning them into pGL3P (F5 and R3) are shown by arrows. The length of each exon is not drawn to scale. (B) Nucleotide sequence of the 5′-UTR of the *DLG1* gene. The previously reported TSS (G) is marked as +1 with a bent arrow (GeneBank ID U13896 and U13897) [35]. Numbers on the left show bases upstream (–) and downstream (+) from the above specified TSS. The extra exon B is shown as a shaded area. The splice junctions (nucleotides AG in the splice acceptor site and GT in the donor site) are indicated in bold. The 3′ and 5′ splice site on the exon sequences are underlined (GT and CG, respectively). The uATG and the main translation start ATG are shown by boxes with continued and dotted lines, respectively. The uORF stop codon TAG is underlined and shown in italics. (C) RT-PCR analysis of both DLG1 5′-UTRs. Total RNA of the indicated cell lines was extracted and subjected to RT-PCR. Both large and short 5′-UTR forms of DLG1 are shown as upper and lower bands respectively.

transiently transfected into HEK293 cells. Renilla-normalized LUC activity for each construct was compared with the insertionless pGL3P (promoter control) and expressed in Fig. 2B as relative firefly luciferase activity. As shown in Fig. 2B, the results of these assays showed conclusively that there were significant differences in LUC activity between the constructs. The normalized LUC activity values were 2.3 and 0.66 in cells transfected with either the pGL3P-5′-UTR short construct or the pGL3P-5′-UTR large plasmid, respectively. Therefore the relative luciferase activity in cells transfected with the pGL3P-5′-UTR short construct was nearly three-fold higher than that from cells transfected with the large version.

To investigate the mechanism that might be responsible for these differences in translation levels, we examined the contribution of the previously identified uORF, since uORFs can reduce the translational efficiency of a subsequent reading frame by stopping a proportion of the scanning ribosomes from reaching the true start codon [37]. Thus, we investigated whether the presence of the uORF in the 5′-UTR

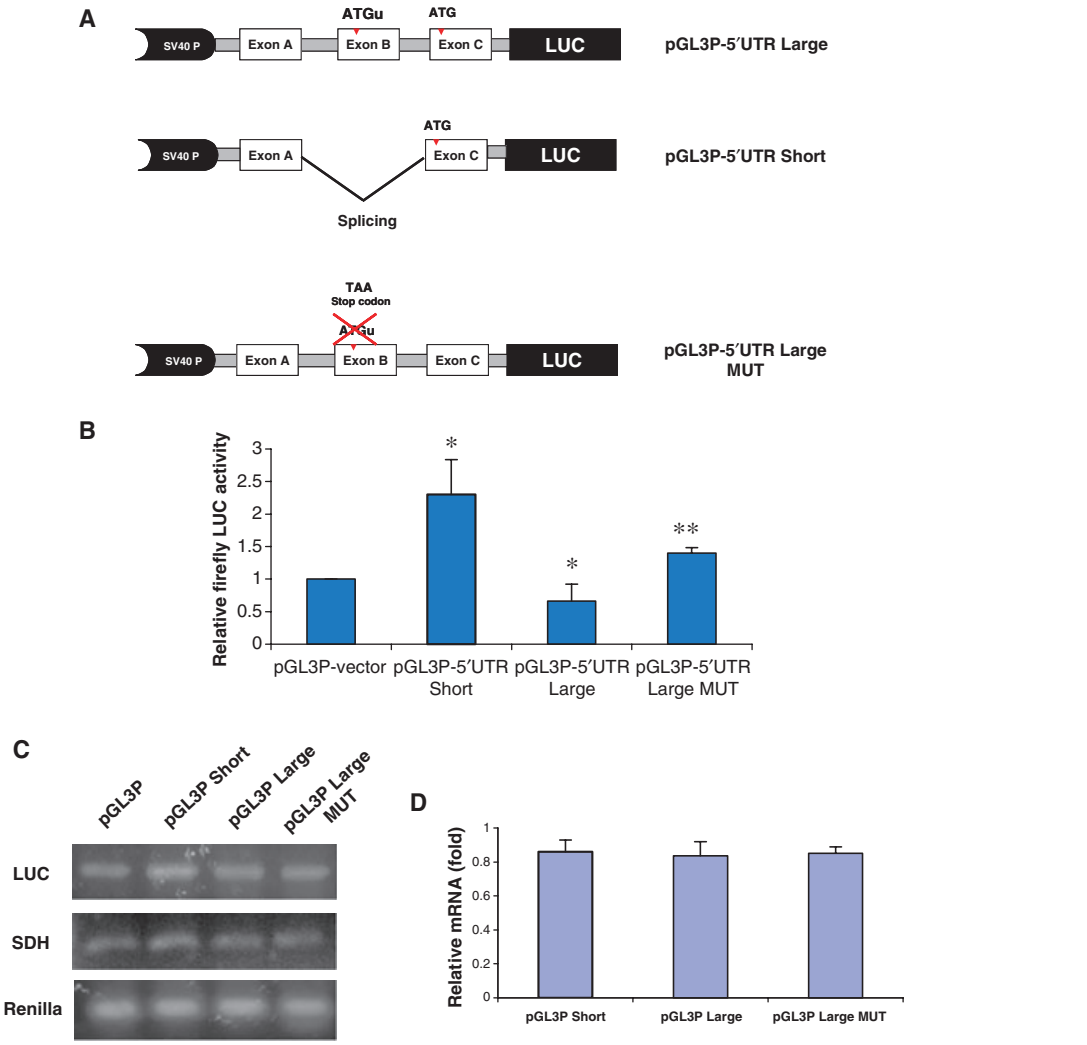

Fig. 2. 5′-UTRs of DLG1 determine translation efficiency. (A) Schematic representation of DLG1 5′-UTR reporter constructs. LUC reporter gene constructs were designed to contain individual 5′-UTRs upstream of the LUC reporter gene in the pGL3P vector (Promega): pGL3P-5′-UTR large (containing exons A, B and C); pGL3P-5′-UTR short (lacking exon B) and pGL3P-5′-UTR large MUT (containing the uATG mutated to a stop codon: ATG → TAA). (B) Effect of DLG1 mRNA 5′-UTRs upon LUC activity. The different reporter plasmids (0.04 μg) were transfected into HEK293T cells. The level of LUC was normalized with the internal Renilla control (0.004 μg). The bars show normalized LUC activity relative to the pGL3P vector data which was arbitrarily considered to be 1. Results represent data from three independent experiments, each performed in triplicate. Mean data ± standard errors are shown. $*P < 0.005$ pGL3P-5′-UTR short versus pGL3P-5′-UTR large relative LUC activity. $**P < 0.05$ pGL3P-5′-UTR large MUT versus pGL3P-5′-UTR large relative LUC activity. (C),(D) Differences in LUC activity did not result from variations in LUC transcription. (C) cDNA fragments for LUC (upper panel), SDH (middle panel) and Renilla luciferase (lower panel) were specifically amplified by RT-PCR from HEK293 cells transfected with the different pGL3P-5′-UTR reporter vectors. The levels of SDH were analysed as a control of the amount of cDNA. The levels of Renilla were analysed as an internal control for normalization of transfection efficiency. (D) For quantification we performed RT-qPCR as described in Materials and methods. The LUC mRNA contents were normalized to the SDH mRNA contents for all samples and the relative LUC mRNA for pGL3P (empty vector) was arbitrarily considered to be 1 (control).

DLG1 large affects the efficiency of translation of the LUC downstream ORF. To test this, we mutated the uATG to a stop codon (TAA) in the pGL3P-5′-UTR large vector and analysed effects on LUC expression. This mutation allowed the generation of a third reporter vector, called as pGL3P-5′-UTR large MUT (Fig. 2A), which was transfected into HEK293 cells. As can be seen in Fig. 2B, this mutated vector showed a substantial increase in reporter activity compared with the wild-type form, and in line with the above predictions; however, the levels were restored only to 60% of the levels of the short form. This observation

was in agreement with previous reports that suggest the involvement of multiple mechanisms affecting translation efficiency [31]. Nevertheless, the data presented in Fig. 2B clearly suggest that the mutation of the uATG in the large version of 5′-UTR DLG1 was able to increase translation efficiency of the downstream ORF, indicating that the presence of a uATG in the exon-B-included 5′-UTR variant decreases the initiation efficiency of the ATG preceding the main ORF (start ATG).

To ensure that these differences in LUC activity did not result from variations in LUC transcription, we performed semiquantitative RT-PCR and real-time quantitative RT-PCR (RT-qPCR) analysis (Fig. 2C,D). Human succinate dehydrogenase (SDH) RNA was used as an endogenous control for assessment of relative amounts of overall cDNA template. These assays showed no differences in LUC mRNA levels between cells transfected with the different pGL3P-5′-UTR reporter vectors. Similar rates of LUC mRNA showed also that there are no significant differences in the amounts of input plasmid or in their transfection efficiencies. It is clear then that differences in transcription from these vectors do not account for the differences in protein expression, and that therefore the inclusion of exon B in the large 5′-UTR must have diminished translation of the downstream LUC ORF. This indicates that DLG1 5′-UTR specifies the efficiency with which downstream ORFs are translated.

As noted above, differential expression of alternative 5′-UTRs can be found in different tissues and has been linked with tumour progression [31]. Therefore, we wanted to investigate if previously reported changes in DLG1 levels in cancer cells and tissues could be related to differential expression of alternative DLG1 5′-UTRs [15,16,38]. To do this we performed RT-qPCR analyses of the expression of short and large DLG1 5′-UTR on cDNA isolated from immortal and transformed epithelial cells. Interestingly, the short DLG1 5′-UTR was upregulated in the immortalized cells relative to transformed cells, in both the squamous (immortal HaCaT with respect to tumourigenic C33A, Fig. S1A) and kidney (immortal HK-2 with respect to transformed HEK293, Fig. S1B) derived cell lines. This result, whilst preliminary, suggests that the short and the large DLG1 5′-UTRs are differentially expressed between cells with different degrees of malignant progression.

Role of the different DLG1 5′-UTRs in mRNA stability

The data described above suggested that the alternative splicing event in the DLG1 5′-UTR can contribute to the regulation of DLG1 expression efficiency. Since it has been reported that the 5′-UTR can affect the stability of mRNA [34], we next wanted to examine whether the different 5′-UTRs modulate DLG1 message stability. To do this, cells were treated with actinomycin D in order to halt synthesis of mRNA. Cells were incubated with actinomycin D for up to 6 h, and cDNA was prepared at various times as indicated in Fig. 3. We performed semiquantitative and RT-qPCR analysis using primers for each specific UTR, for a sequence from the DLG1 reading frame (which is present in all DLG1 messages) and for SDH, to allow assessment of relative amounts of overall cDNA template. The specificity of the qPCR amplification was documented, in addition to melting curve analysis, with agarose gel electrophoresis, revealing a single product with the expected size in each case (data not shown). The results obtained by the two methods revealed no significant differences in mRNA stability among the DLG1 5′-UTR variants. As can be seen in Fig. 3A,B, mRNA containing both forms of DLG1 5′-UTR, large and short, remained at considerable

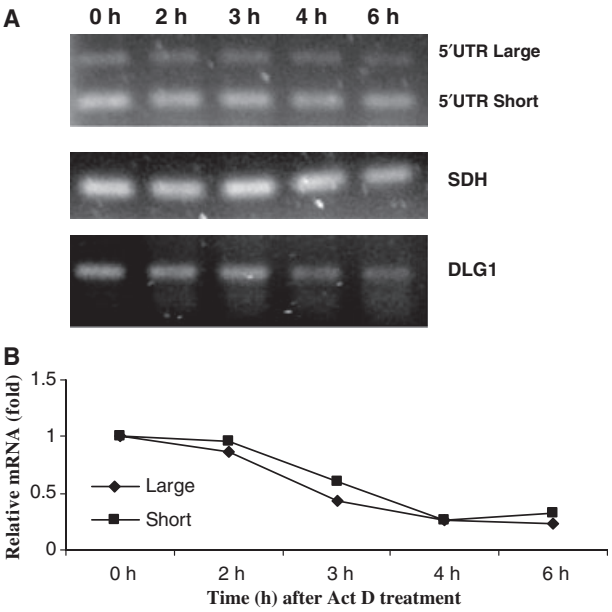

Fig. 3. Role of the different DLG1 5′-UTRs in mRNA stability. HaCaT cells were treated with actinomycin D (5 $\mu g \cdot mL^{-1}$) and the total RNAs were prepared and processed at the indicated time points. (A) RT-PCR analysis of each alternative DLG1 5′-UTR, total DLG1 and SDH were performed as described in Materials and methods. The levels of SDH were analysed as a control of the amount of cDNA. (B) For quantification we performed RT-qPCR as described in Materials and methods. The DLG1 5′-UTR mRNA contents were normalized to the SDH mRNA contents for all samples and the relative DLG1 5′-UTR mRNA at 0 h was arbitrarily considered to be 1 (control).

levels after 6 h of treatment with the inhibitor, indicating that they are relatively stable. These stabilities are reflected in the stability of total DLG1 mRNA (Fig. 3A). We conclude that an accelerated degradation of mRNA probably does not contribute to the observed reduction in reporter gene expression associated with the DLG1 5′-UTR large, and that the alternative splicing event in the DLG1 5′-UTR does not influence the stability of mRNA.

RNA fold modelling

Secondary structure within 5′-UTR can strongly influence translational efficiency by acting as binding sites for some regulatory proteins or by inhibiting the binding or scanning of the translational machinery [27]. Then, we were interested in whether RNA secondary structure within these UTRs could contribute to the differences in translation efficiency for each splice variant. Recent advances in computational modelling of DNA and RNA have made such an investigation a viable approach.

We have examined whether DLG1 5′-UTRs are capable of forming significant secondary structure. Using the MFOLD RNA-folding software [39], each splice variant's mRNA sequence was computationally folded. The degree and stability of these structures can be quantified using the theoretical change in free energy (ΔG); structures that are more stable release more energy and have greater ΔG values. DLG1 5′-UTR large can form a structure with a ΔG value of −90 kcal·mol^{-1}, whereas the ΔG value of the DLG1 5′-UTR short is only −30 kcal·mol^{-1} (Fig. 4). Modelling also revealed that the 115 additional nucleotides of exon B, present in the large version of DLG1 5′-UTR, can form an extremely stable stem loop (ΔG, −55 kcal·mol^{-1}) (data not shown). These data indicate that the large form of DLG1 5′-UTR contains a significant secondary structure that may well contribute to its low translation efficiency, validating the results obtained with the LUC assays. Interestingly, RNA modelling also showed that the secondary structure of the 5′-UTR large was maintained for the 5′-UTR large MUT version bearing a mutation of the uATG (ΔG −89 kcal·mol^{-1} for 5′-UTR large MUT, Fig. 4). Thus, the combinations of uORFs with stable secondary structures in the DLG1 5′-UTR large are likely to have a role as mediators of the observed patterns of translation.

Discussion

In this study we present new insights about the mechanisms that regulate DLG1 expression. Although several alternatively spliced DLG1 isoforms have been previously described, those splicing events occur solely in the DLG1 coding region [40]. Thus, this is the first report demonstrating that the *DLG1* gene undergoes alternative splicing to give two different transcripts containing distinct 5′-UTRs (large and short).

Since DLG1 is known to be altered in cancers of epithelial origin and is the target of oncogenic HPV, we were first interested in investigating the initiation of DLG1 transcription in epithelial cells [15,16]. The results of RACE assays using HaCaT epithelial cells allowed the identification of several initiation sites. Transcription from multiple start sites that are often distributed over a short region of about 100 nucleotides has been proposed for TATA-less promoters rich in GC box motifs, such as the DLG1 promoter [26]. However, it is not possible to rule out the possibility that some of the RACE sequenced products might be truncated forms. As previously mentioned, the original published cDNA reported by Lue *et al.* [35] (GeneBank ID U13896 and U13897), and also a second published sequence concerning the DLG1 IS2 isoform (GeneBank ID NM_004087), designated the G nucleotide shown as +1 (Fig. 1A,B) as the TSS. The sequence of these entries coincides exactly with the large 5′-UTR DLG1 that we identified. A BLASTN search of human expressed sequence tags databases using the published cDNA sequences revealed many expressed sequence tags that share homology with DLG1 but which differ from the classical sequence in the 5′ end (GeneBank ID U13896 and U13897) [35]. This provides evidence that DLG1 transcripts with variable 5′ termini probably exist. Interestingly, a significant number of those DLG1 sequences with different 5′-UTRs came from placental or fetal tissues. This analysis was confirmed by bioinformatics data obtained using the UTR database tool developed by Grillo *et al.* [41] (http://utrdb.ba.itb.cnr.it/). In this case, six different entries were found for the DLG1 5′-UTR. Four of them corresponded to the original published cDNA mentioned above (GeneBank ID U13896 and U13897, [35]). The other entries corresponded to cDNA with unusual 5′-UTRs in the DLG1 transcripts and were derived from fetal liver (GeneBank ID EF553524) and placenta (GeneBank ID BC015560). Future analysis using RNA from different tissues will help to confirm these sequences and confirm the regulation of DLG1 expression by these alternative 5′-UTR isoforms.

We have functionally analysed the large and short DLG1 5′-UTRs and found that 5′ end shortening as well as skipping of exon B increased the capacity for heterologous protein expression (Fig. 2B). The *in vivo*

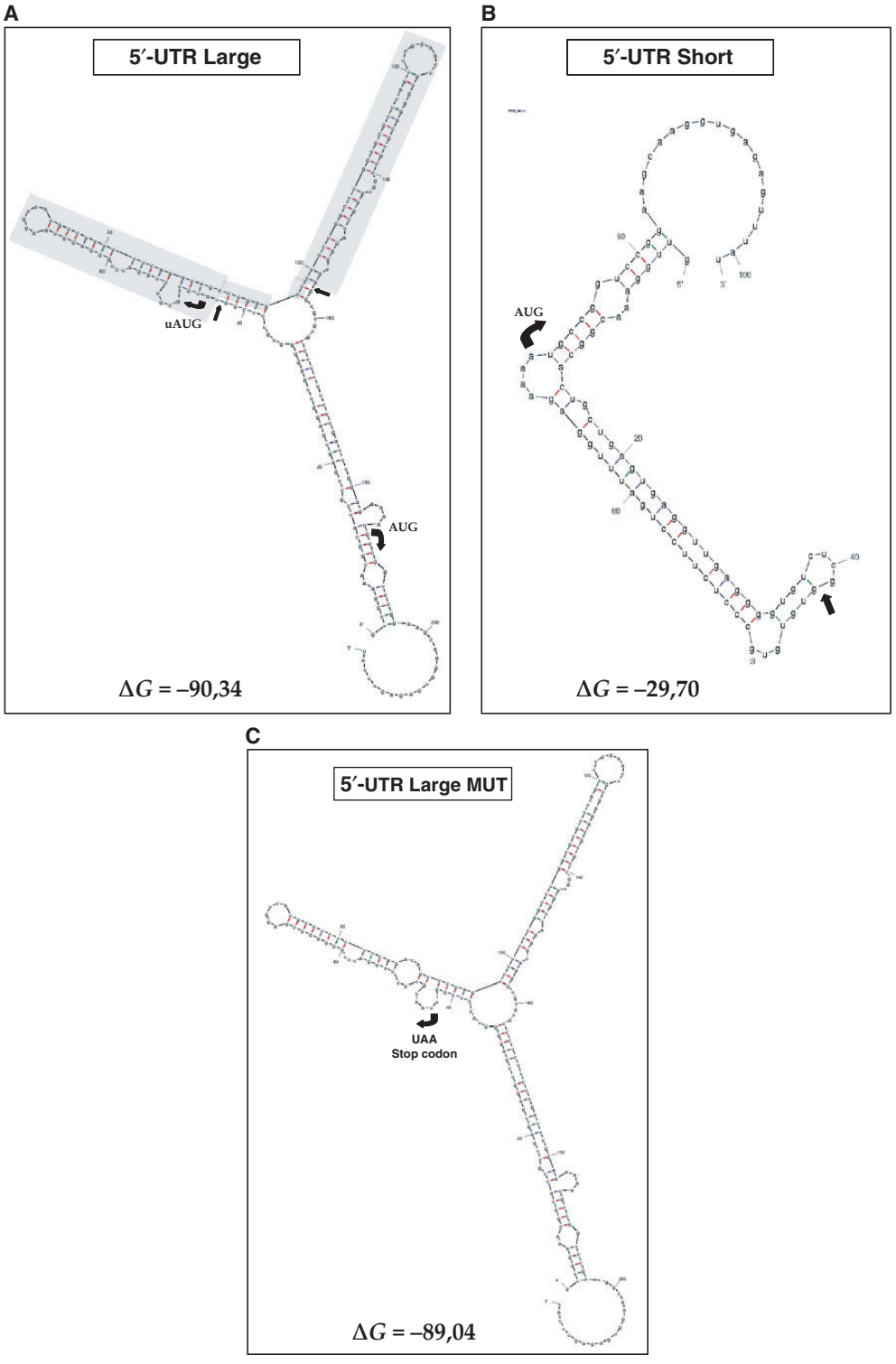

Fig. 4. Secondary structure of DLG1 5′-UTR large and short mRNA. Bent arrows indicate the start of the ORFs (uATG and ATG). The shaded area in the left panel corresponds to the 115 nucleotide sequence that is spliced out in DLG1 5′-UTR short. The splice junction is indicated by straight arrows. The mutation of the uATG to a stop codon in the 5′-UTR DLG1 large MUT is indicated (bottom panel).

experiments using LUC reporter gene assays indicated that translational efficiency of the short 5′-UTR is higher than that of the exon-B-containing 5′-UTR version. Moreover, this difference may be due to post-transcriptional mechanisms rather than to differences in the transcription activity (Fig. 2C). These observations are in line with previous suggestions that shorter 5′-UTRs are more capable of efficient translation [42], and support the notion that alternative events in 5′-UTRs of mammalian genes contribute to the regulation of translation. It is important to note that the DLG1 large and short 5′-UTRs, cloned into the reporter vector (pGL3P), are represented by transcripts bearing a common TSS found in 5′ RACE clones and shared by the two isoforms (nucleotide −11, Fig. 1A).

There are several mechanisms by which the 5′-UTR may regulate translation. Stable secondary structures and the presence of the short uORF in the 5′-UTR considerably compromise translation efficiency [32]. While moving along the transcript, the 40 S ribosomal subunit scans and evaluates initiation codons sequentially, starting at the 5′ end of the mRNA. The presence of short ORFs in the 5′-UTR allows the initiation complex to remain bound to the RNA even after the apparently wasteful translation of the short peptide. Thus, a small ORF greatly reduces but does not eliminate translation of the correct polypeptide [43]. We have examined whether such mechanisms are involved in the differences observed in translation efficiency mediated by the alternative DLG1 5′-UTR. We have identified in the alternative spliced exon the presence of a small uORF (seven codons) and demonstrated that mutation of the uATG could reverse to some extent the negative regulation of the large 5′-UTR.

It has been demonstrated that 5′-UTRs can regulate mRNA stability and specifically that RNA decay is enhanced in uORF-containing transcripts, contributing towards the low translation efficiency [44]. Thus, we investigated the decay rate of DLG1 RNA bearing the different DLG1 5′-UTRs by treatment with actinomycin D and RT-PCR assays. We found in this case that there was no significant difference in the stabilities of the two 5′-UTR isoforms and the relative low decay rate is reflected in the levels of the coding DLG1 mRNA region used as a control. This observation is in line with reports indicating that mRNA stability is regulated by the 3′-UTR rather than the 5′ termini of the transcripts [45].

Secondary stem loop structures in the 5′-UTR have been shown to block the migration of 40 S ribosomes during translation, especially for stable structures ($\Delta G < -50$ kcal·mol^{-1}) [32]. In some cases trans-acting factors bind these elements and regulate continued scanning of the ribosome; in others, the RNA structure itself blocks ribosome passage [46]. Using computational modelling we showed that the large DLG1 5′-UTR isoform forms a more stable structure than the short version. This altered secondary structure might result in loss/gain of recognition by specific cellular factors, thus potentially contributing to the differential translation efficiency of the isoforms. The stable structure was conserved even when the uORF was disrupted (Fig. 4), which could explain why the mutated version of the large 5′-UTR, whilst restoring the efficiency of translation, was still less efficient than the short version (Fig. 2B). Again these data demonstrate that multiple mechanisms contribute to the regulation of translation mediated by the 5′-UTR, including the presence of uORF and RNA secondary structures, which is similar to recent findings reported by Smith and collaborators [31]. It has also been previously reported that the 3′-UTR can play a role in the regulation of translation, and that specific combinations of alternative 5′- and 3′-UTRs can specify the efficiency of translation of individual transcripts [31]. To our knowledge, the cloning, analysis and/or identification of alternatively expressed DLG1 3′-UTRs have so far not been reported. This is an interesting aspect that needs to be taken into consideration in future studies for gaining a more complete understanding of the regulation of DLG1 expression.

There are many examples in which non-coding elements within messages modify gene expression [37,47]; however, very few studies have shown physiological regulation with alternative UTRs that, in turn, allow the synthesis of different amounts of protein. Most of the studies show genes deregulated in this way during carcinogenesis [30,31,46].

Here we describe a further mechanism by which the tumour suppressor activities of DLG1 may be regulated: downregulation of DLG1 by modulation of the relative expression of DLG1 5′-UTRs. Furthermore, having shown that these 5′-UTRs have differential effects on translational efficiency, future work to analyse if the alternative 5′-UTRs are differentially expressed between various normal and tumour tissues would help towards an understanding of the changes in DLG1 abundance during tumour progression [15,16]. As a preliminary step towards this, we in fact showed by RT-qPCR analysis that the large DLG1 5′-UTR isoform, which reduces the translation efficiency of a downstream ORF, is indeed upregulated in cells with a greater degree of malignant potential (Fig. S1).

In summary, we have demonstrated that the DLG1 transcript can be expressed with an alternatively spliced 5′-UTR, and that the different 5′-UTRs directly

regulate the translation of the downstream ORF. We have also determined that uORFs and stable secondary structures are responsible for this regulation. Thus, DLG1 expression may be defined not only by the total amount of mRNA but also by the proportions of the different 5′-UTRs within these messages, allowing the fine tuning of DLG1 expression according to the physiological requirements of the cell.

Materials and methods

Cell culture and transfections

Human embryonic kidney (HEK293), HaCaT, HeLa, C33A, HK-2 and CaCo-2 cells were grown in Dulbecco's modified Eagle's medium (Gibco, Grand Island, NY, USA) supplemented with 10% fetal bovine serum (Gibco). Cells were transfected using calcium phosphate precipitation as described previously [48].

RNA isolation, cDNA synthesis, semiquantitative RT- PCR and real-time RT-PCR

Total RNA was purified using Trizol according to the manufacturer's protocol (Invitrogen, Carlsbad, CA, USA). For evaluating the levels of chimeric luciferase transcripts, RNA was purified using the NucleoSpin RNA/Protein kit (Macherey-Nagel, Düren-Düren, Germany) that includes a treatment with DNase in order to avoid the amplification of reporter plasmid DNA. Synthesis of cDNA was obtained from 2 μg of RNA using 200 U MMLV reverse transcriptase (Invitrogen) and either random hexamers or oligo(dT) primers. A control lacking reverse transcriptase was also performed. cDNA samples were subjected to PCR using specific primer pairs. Each alternative DLG1 5′-UTR was amplified specifically using different sense primers corresponding to sequences across the A/B exon boundary (F3, for DLG1 5′-UTR large 5′-TGTCTCGGTATGTGCGCCTT-3′) or the A/C exon boundary (F4, for DLG1 5′-UTR short, 5′-TGTCTCGGTGTGTGCCCTCTT-3′) and a common antisense primer (R, 5′-AGCTGTCTGTCTTCAGTTTGGCT-3′) derived from sequences in exon C. The localization of these primers is shown in Fig. 1A. Total DLG1 cDNA was amplified using primers that target the coding region [DLG-F, 5′-CAAGCAGCCTTAGCCCTAGTGTA-3′ (sense), and DLG-R, 5′-CATGAACCAATTCTGGACCTATCA-3′ (antisense)]. SDH, used as housekeeping marker, was amplified with SDH-F 5′-GCACACCCTGTCCTTTGT-3′ (sense) and SDH-R 5′-CACAGTCAGCCTCGTTCA-3′ (antisense) oligonucleotides. Firefly luciferase (LUC, used as control to ensure that the differences in LUC activity were not due to variations in firefly LUC mRNA expression) was amplified with primers LucF 5′-TCAAAGAGGCGAACTGTGTG-3′ (sense) and LucR 5′-GGTGTTGGAGCAAGTGGAT-3′ (antisense); and Renilla luciferase (used as internal control for normalization of transfection efficiency) with RL-Fw 5′-ATGGGATGAATGGCCTGATA-3′ (sense) and RL-Rv 5′-CAACATGGTTTCCACGAAGA-3′ (antisense) oligonucleotides.

To investigate the stability of the DLG1 mRNAs, HaCaT cells were treated with actinomycin D (5 $\mu g \cdot mL^{-1}$) and harvested at 0, 2, 3, 4 and 6 h post addition of the drug, when total RNA was isolated and processed as described above.

RT-qPCR analysis was performed using Eva Green qPCR Mezcla Real (Biodynamics, Buenos Aires, Argentina) and Eppendorf Mastercycler EP Realplex (Eppendorf, Hamburg, Germany). For these analyses, the primers used were the same as described above except for DLG1 5′-UTR large transcript where a new sense primer was designed with the following sequence: F-large, 5′-GGGCTAGGGCAAGGTGTGT-3′. All qPCR runs were done using the following conditions: 5 min at 95 °C followed by 40 cycles of denaturation (15 s at 95 °C), annealing (15 s at 57 °C) and extension (20 s at 68 °C), with a single acquisition of fluorescence levels at the end of each extension step. Melting curves were generated after each PCR to maximize fluorescence from Eva Green binding to the desired amplicon and to ensure that a single, specific product was amplified. The specificity of the amplified PCR products was also confirmed by agarose gel electrophoresis. The results were analysed with the comparative cycle threshold method. All experiments were carried out in triplicate and repeated at least four times.

5′-RACE-PCR

TSSs of DLG1 were mapped by 5′-RACE-PCR. Total HaCaT cell RNA was prepared as described. The 5′-RACE-PCR products were generated using the First Choice RLMR ACE kit following the manufacturer's instructions (Ambion, Austin, TX, USA). Briefly, dephosphorylated and de-capped HaCaT mRNAs were ligated to the RLMRACE RNA oligo (Ambion). Then, cDNAs were synthesized using random hexamers as described. The single-stranded cDNAs were amplified in a primary PCR with adaptor primer RLMR ACE 5′ RACE Outer 5′ (5′-GCTGATGGCGATGAAT GAACACTG-3′) and the gene specific reverse primer 3′-DLG Outer (5′-TCCTCCAAAAGGTGCAATGCTCT CT-3′), followed by a secondary PCR using the nested adaptor primer RLMRACE 5′ RACE Inner 5′ (5′-CG CGGATCCGAACACTGCGTTTGCTGGCTTTGATG-3′) and the gene specific reverse primer 3′-DLG Inner (5′-TC CGGACCGGCATTTTTCTCCAGAA-3′). Specific DLG1 primers were designed according to the reported DLG1 cDNA sequences and correspond to sequences in exon C close to the initiation of translation (Fig. 1A) [35]. The conditions for the first- and second-round PCRs consisted of 5 min at 94 °C, 30 cycles of 94 °C for 30 s, 62 °C for 30 s

and 72 °C for 30 s, with a final extension of 10 min at 72 °C. PCR products were separated on a 1.5% agarose gel, purified and cloned into pGEM-T Easy plasmid (Promega). Insert DNAs were isolated from individual colonies and sequenced.

Plasmid construction

For construction of the reporter gene vectors, the alternative 5′-UTR of DLG1 transcripts were PCR amplified by using specific RACE products as templates, and primers DlgF5 [5′- TATAAGCTTT(-11)CTGCCGCGGAGTTGGAAA-3′ (sense)] and DLGR3 [5′-TATCCATGGTTCTCCAGAA TCGAGGAAGAGG-3′ (antisense)], which contain the *Hind*III and *Nco*I restriction sites respectively (underlined), to facilitate cloning into the pGL3P luciferase reporter vector (Promega). The primer locations are shown in Fig. 1A. After amplification, the PCR products were digested with *Hind*III and *Nco*I, gel purified and cloned into the pGEM-T Easy vector. The identities of the clones for the large and short 5′-UTRs were confirmed by sequencing analysis. Inserts from positive clones were removed by digestion with *Hind*III and *Nco*I and subcloned into *Hind*III/*Nco*I digested pGL3P luciferase reporter vector (Promega). The 5′-UTRs were inserted upstream of LUC ORF, which is under the control of the SV40 early enhancer/promoter. The *Nco*I site hence contains the initiating ATG of LUC, excluding any vector-derived 5′-UTR sequence. The DLG1 5′-UTR large MUT construct was obtained by introducing point mutations into the upstream ATG (uATG, ATG → TAA) by the two-step PCR method described by Higuchi [49]. The primers used were 5′-TGTCTCGGTTAATGCGCCTTGGATCTGGTGTAGG CGAGGT-3′ (sense) and 5′-ACCTCGCCTACACCAGATC CAAGGCGCATTAACCGAGACA-3′ (antisense). The mutated fragment was inserted into *Hind*III/*Nco*I digested pGL3P vector, as described above. All the derivatives were confirmed by DNA sequencing.

Measurement of luciferase activity

The translational efficiency for each 5′-UTR was measured with reporter gene constructs using the dual luciferase reporter assay kit from Biotium (Hayward, CA, USA). HEK293 cells were cultured overnight and transfected with the different chimeric pGL3P constructs. For normalization of transfection efficiency, the pRL vector encoding Renilla luciferase was co-transfected as internal control and the level of LUC was normalized to that of the Renilla luciferase activity in each experiment. For all experiments, cells were cultured for 24–48 h after transfection, luciferase assays were performed using the Firefly & Renilla Luciferase Assay Kit, and luminescence was measured on a luminometer LD 400 (Beckman Coulter, Brea, CA, USA). The data from the luciferase experiments were then compared with the activity of the insertion-less pGL3P (designed promoter control), and LUC activity was expressed as an *n*-fold increase in activity. All experiments were carried out in triplicate and repeated at least four times.

Modelling of RNA secondary structure

Modelling of the secondary structures of the different splice variant mRNAs was performed using the MFOLD program (version 3.2) developed by Zuker [39]. The portal for the MFOLD web server is http://www.bioinfo.rpi.edu/applications/mfold. The mRNA sequences were simulated as though they were at 37 °C in 1 M NaCl, which is the current standard condition used in fold modelling.

Statistical analysis

The statistical significance of the data from the luciferase assays was obtained by analysis of variance (ANOVA), followed by multiple comparisons performed by the Duncan test. A P value < 0.05 was considered significant.

Acknowledgements

We gratefully acknowledge Dr Luciano D'Attilio (Facultad de Ciencias Médicas, Universidad Nacional de Rosario) for helpful advice and discussion of the work. We also acknowledge to Dolores Campos for valuable technical support. This work was supported in part by research grants from the Agencia de Promoción Científica y Tecnológica (Argentina, PICT 05-25464, PICT 2008-0421) and by the Associazione Italiana per la Ricerca sul Cancro.

References

1 Humbert P, Russell S & Richardson H (2003) Dlg, Scribble and Lgl in cell polarity, cell proliferation and cancer. *Bioessays* **25**, 542–553.
2 Kim SK (1997) Polarized signaling: basolateral receptor localization in epithelial cells by PDZ-containing proteins. *Curr Opin Cell Biol* **9**, 853–859.
3 Bilder D (2004) Epithelial polarity and proliferation control: links from the Drosophila neoplastic tumor suppressors. *Genes Dev* **18**, 1909–1925.
4 Caruana G (2002) Genetic studies define MAGUK proteins as regulators of epithelial cell polarity. *Int J Dev Biol* **46**, 511–518.
5 Goode S & Perrimon N (1997) Inhibition of patterned cell shape change and cell invasion by Discs large during Drosophila oogenesis. *Genes Dev* **11**, 2532–2544.
6 Reuver SM & Garner CC (1998) E-cadherin mediated cell adhesion recruits SAP97 into the cortical cytoskeleton. *J Cell Sci* **111**, 1071–1080.
7 Laprise P, Viel A & Rivard N (2004) Human homolog of disc-large is required for adherens junction assembly

and differentiation of human intestinal epithelial cells. *J Biol Chem* **279**, 10157–10166.
8 Assemat E, Bazellieres E, Pallesi-Pocachard E, Le Bivic A & Massey-Harroche D (2008) Polarity complex proteins. *Biochim Biophys Acta* **1778**, 614–630.
9 Ishidate T, Matsumine A, Toyoshima K & Akiyama T (2000) The APC-hDLG complex negatively regulates cell cycle progression from the G0/G1 to S phase. *Oncogene* **19**, 365–372.
10 Lee SS, Weiss RS & Javier RT (1997) Binding of human virus oncoproteins to hDlg/SAP97, a mammalian homolog of the Drosophila discs large tumor suppressor protein. *Proc Natl Acad Sci USA* **94**, 6670–6675.
11 Gardiol D, Kuhne C, Glaunsinger B, Lee SS, Javier R & Banks L (1999) Oncogenic human papillomavirus E6 proteins target the discs large tumour suppressor for proteasome-mediated degradation. *Oncogene* **18**, 5487–5496.
12 Suzuki T, Ohsugi Y, Uchida-Toita M, Akiyama T & Yoshida M (1999) Tax oncoprotein of HTLV-1 binds to the human homologue of Drosophila discs large tumor suppressor protein, hDLG, and perturbs its function in cell growth control. *Oncogene* **18**, 5967–5972.
13 Gardiol D, Galizzi S & Banks L (2002) Mutational analysis of the discs large tumour suppressor identifies domains responsible for human papillomavirus type 18 E6-mediated degradation. *J Gen Virol* **83**, 283–289.
14 Kuhne C, Gardiol D, Guarnaccia C, Amenitsch H & Banks L (2000) Differential regulation of human papillomavirus E6 by protein kinase A: conditional degradation of human discs large protein by oncogenic E6. *Oncogene* **19**, 5884–5891.
15 Cavatorta AL, Fumero G, Chouhy D, Aguirre R, Nocito AL, Giri AA, Banks L & Gardiol D (2004) Differential expression of the human homologue of drosophila discs large oncosuppressor in histologic samples from human papillomavirus-associated lesions as a marker for progression to malignancy. *Int J Cancer* **111**, 373–380.
16 Gardiol D, Zacchi A, Petrera F, Stanta G & Banks L (2006) Human discs large and scrib are localized at the same regions in colon mucosa and changes in their expression patterns are correlated with loss of tissue architecture during malignant progression. *Int J Cancer* **119**, 1285–1290.
17 Boussioutas A, Li H, Liu J, Waring P, Lade S, Holloway AJ, Taupin D, Gorringe K, Haviv I, Desmond PV *et al.* (2003) Distinctive patterns of gene expression in premalignant gastric mucosa and gastric cancer. *Cancer Res* **63**, 2569–2577.
18 Fuja TJ, Lin F, Osann KE & Bryant PJ (2004) Somatic mutations and altered expression of the candidate tumor suppressors CSNK1 epsilon, DLG1, and EDD/hHYD in mammary ductal carcinoma. *Cancer Res* **64**, 942–951.
19 Watson RA, Rollason TP, Reynolds GM, Murray PG, Banks L & Roberts S (2002) Changes in expression of the human homologue of the Drosophila discs large tumour suppressor protein in high-grade premalignant cervical neoplasias. *Carcinogenesis* **23**, 1791–1796.
20 Massimi P, Narayan N, Cuenda A & Banks L (2006) Phosphorylation of the discs large tumour suppressor protein controls its membrane localisation and enhances its susceptibility to HPV E6-induced degradation. *Oncogene* **25**, 4276–4285.
21 Sabio G, Arthur JS, Kuma Y, Peggie M, Carr J, Murray-Tait V, Centeno F, Goedert M, Morrice NA & Cuenda A (2005) p38gamma regulates the localisation of SAP97 in the cytoskeleton by modulating its interaction with GKAP. *EMBO J* **24**, 1134–1145.
22 Gaudet S, Branton D & Lue RA (2000) Characterization of PDZ-binding kinase, a mitotic kinase. *Proc Natl Acad Sci USA* **97**, 5167–5172.
23 Narayan N, Massimi P & Banks L (2009) CDK phosphorylation of the discs large tumour suppressor controls its localisation and stability. *J Cell Sci* **122**, 65–74.
24 Mantovani F & Banks L (2001) The human papillomavirus E6 protein and its contribution to malignant progression. *Oncogene* **20**, 7874–7887.
25 Peinado H, Olmeda D & Cano A (2007) Snail, Zeb and bHLH factors in tumour progression: an alliance against the epithelial phenotype? *Nat Rev Cancer* **7**, 415–428.
26 Cavatorta AL, Giri AA, Banks L & Gardiol D (2008) Cloning and functional analysis of the promoter region of the human Disc large gene. *Gene* **424**, 87–95.
27 Hughes TA (2006) Regulation of gene expression by alternative untranslated regions. *Trends Genet* **22**, 119–122.
28 Pesole G, Mignone F, Gissi C, Grillo G, Licciulli F & Liuni S (2001) Structural and functional features of eukaryotic mRNA untranslated regions. *Gene* **276**, 73–81.
29 Cenik C, Derti A, Mellor JC, Berriz GF & Roth FP (2010) Genome-wide functional analysis of human 5′ untranslated region introns. *Genome Biol* **11**, R29.
30 Smith L (2008) Post-transcriptional regulation of gene expression by alternative 5′-untranslated regions in carcinogenesis. *Biochem Soc Trans* **36**, 708–711.
31 Smith L, Brannan RA, Hanby AM, Shaaban AM, Verghese ET, Peter MB, Pollock S, Satheesha S, Szynkiewicz M, Speirs V *et al.* (2010) Differential regulation of oestrogen receptor beta isoforms by 5′ untranslated regions in cancer. *J Cell Mol Med* **14**, 2172–2184.
32 Kozak M (1991) Structural features in eukaryotic mRNAs that modulate the initiation of translation. *J Biol Chem* **266**, 19867–19870.

33 Pesole G, Grillo G, Larizza A & Liuni S (2000) The untranslated regions of eukaryotic mRNAs: structure, function, evolution and bioinformatic tools for their analysis. *Brief Bioinform* **1**, 236–249.
34 Mignone F, Gissi C, Liuni S & Pesole G (2002) Untranslated regions of mRNAs. *Genome Biol* **3**, REVIEWS0004.1-0004.10.
35 Lue RA, Marfatia SM, Branton D & Chishti AH (1994) Cloning and characterization of hdlg: the human homologue of the Drosophila discs large tumor suppressor binds to protein 4.1. *Proc Natl Acad Sci USA* **91**, 9818–9822.
36 Shimada MK, Hayakawa Y, Takeda J, Gojobori T & Imanishi T (2010) A comprehensive survey of human polymorphisms at conserved splice dinucleotides and its evolutionary relationship with alternative splicing. *BMC Evol Biol* **10**, 122.
37 Meijer HA & Thomas AA (2002) Control of eukaryotic protein synthesis by upstream open reading frames in the 5′-untranslated region of an mRNA. *Biochem J* **367**, 1–11.
38 Mantovani F, Massimi P & Banks L (2001) Proteasome-mediated regulation of the hDlg tumour suppressor protein. *J Cell Sci* **114**, 4285–4292.
39 Zuker M (2003) Mfold web server for nucleic acid folding and hybridization prediction. *Nucleic Acids Res* **31**, 3406–3415.
40 McLaughlin M, Hale R, Ellston D, Gaudet S, Lue RA & Viel A (2002) The distribution and function of alternatively spliced insertions in hDlg. *J Biol Chem* **277**, 6406–6412.
41 Grillo G, Turi A, Licciulli F, Mignone F, Liuni S, Banfi S, Gennarino VA, Horner DS, Pavesi G, Picardi E *et al.* (2010) UTRdb and UTRsite (RELEASE 2010): a collection of sequences and regulatory motifs of the untranslated regions of eukaryotic mRNAs. *Nucleic Acids Res* **38**, D75–D80.
42 Atamna H (2004) Heme, iron, and the mitochondrial decay of ageing. *Ageing Res Rev* **3**, 303–318.
43 Mathews DH, Sabina J, Zuker M & Turner DH (1999) Expanded sequence dependence of thermodynamic parameters improves prediction of RNA secondary structure. *J Mol Biol* **288**, 911–940.
44 Resch AM, Ogurtsov AY, Rogozin IB, Shabalina SA & Koonin EV (2009) Evolution of alternative and constitutive regions of mammalian 5′UTRs. *BMC Genomics* **10**, 162.
45 Barreau C, Paillard L & Osborne HB (2005) AU-rich elements and associated factors: are there unifying principles? *Nucleic Acids Res* **33**, 7138–7150.
46 Stoneley M & Willis AE (2003) Aberrant regulation of translation initiation in tumorigenesis. *Curr Mol Med* **3**, 597–603.
47 Wilkie GS, Dickson KS & Gray NK (2003) Regulation of mRNA translation by 5′- and 3′-UTR-binding factors. *Trends Biochem Sci* **28**, 182–188.
48 Matlashewski G, Schneider J, Banks L, Jones N, Murray A & Crawford L (1987) Human papillomavirus type 16 DNA cooperates with activated ras in transforming primary cells. *EMBO J* **6**, 1741–1746.
49 Higuchi R, Krummel B & Saiki RK (1988) A general method of *in vitro* preparation and specific mutagenesis of DNA fragments: study of protein and DNA interactions. *Nucleic Acids Res* **16**, 7351–7367.

Supporting information

The following supplementary material is available:
Fig. S1. Alternative DLG1 5′-UTRs are differentially expressed in epithelial cells.

This supplementary material can be found in the online version of this article.

Please note: As a service to our authors and readers, this journal provides supporting information supplied by the authors. Such materials are peer-reviewed and may be reorganized for online delivery, but are not copy-edited or typeset. Technical support issues arising from supporting information (other than missing files) should be addressed to the authors.